Heliyon

Trapping and proliferation of target cells on C_{60} fullerene nano fibres

Seiki Iwai [a], Shunji Kurosu [b], Hideki Sasaki [a], Kazunori Kato [b], Toru Maekawa [a],[b],*

[a] *Graduate School of Interdisciplinary New Science, Toyo University, 2100 Kujirai, Kawagoe, Saitama 350-8585, Japan*

[b] *Bio-Nano Electronics Research Centre, Toyo University, 2100 Kujirai, Kawagoe, Saitama 350-8585, Japan*

* Corresponding author.

E-mail address: maekawa@toyo.jp (T. Maekawa).

Abstract

The ratio of the surface area to the volume of materials increases in inverse proportion to their size and therefore the surface area of nanostructures and nanomaterials is extremely large compared to that of macroscopic materials of the same volume, thanks to which it is supposed that chemical and biochemical reactions may be greatly enhanced and target molecules and cells may be efficiently trapped on the surface of nanomaterials. It is well known that C_{60} molecules are stable both physically and chemically and the affinity of C_{60} molecules with biomolecules is rather high. Here, we synthesise fibres composed of C_{60} and sulphur and immobilise the surface of the fibres with the primary antibody; i.e., epithelial cell adhesion molecules (anti-EpCAM), to trap target cells. The primary antibody is evenly immobilised on the fibres confirmed by a fluorescent secondary antibody attached to the primary one and then TE2 esophageal and DLD-1 colon cancer cells are successfully trapped by the primary antibody immobilised on the fibres thanks to its high affinity with TE2 and DLD-1 cells, whereas few IM9 B lymphoblast cells are captured on the fibres since the affinity of the primary antibody with IM9 cells is extremely low. Furthermore, those cells trapped by the primary antibody immobilised on the fibres proliferate faster than native cells thanks to the primary antibody acting as a growth factor. The present result suggests that different types of cells can be trapped and grown on nano fibres by immobilising appropriate antibody molecules on the surface of

the fibres. Even an extremely small number of cells in sample fluids may be analysed and characterised for the detection of diseases such as cancer in the early stage by trapping and proliferating target cells on the fibres.

Keywords: Nanotechnology, Materials science, Biotechnology

1. Introduction

Nanostructures can be formed via so-called bottom-up self-organisation/self-assembly processes as well as top-down ultra-fine ones [1, 2, 3]. Some of the self-organisation/self-assembly methodologies utilise convective patterns formed in liquid solvents [4, 5]. Nano/micro particles, which are dispersed in droplets, are self-assembled to form circular patterns along the circumference of the droplets after evaporation on substrates; known as the coffee-ring effect [6, 7]. Utilisation of nanostructures in the field of biomedicine as well as in the fields of mechanics, electronics, mechatronics and optics has been intensively investigated in recent years [8, 9]. One of the advantageous features in using nanomaterials in the biomedical field is their huge area per unit volume, thanks to which biochemical reactions may be greatly enhanced and the chances of trapping target molecules and cells may be dramatically increased at nanoscales [10, 11]. Nano fibres were used to trap target cancer cells [12, 13, 14], while those were also used as scaffolds for the development of regenerative biomedical materials [13, 15, 16, 17, 18, 19, 20]. However, the synthetic procedure of those nano fibres is quite complicated and the compatibility and affinity of those nanomaterials with biomolecules and cells become a crucial issue [10, 20, 21, 22]. Carbon nanotubes (CNTs) have also been utilised for regenerative medicine, growing cells on the surface of CNTs, and for the development of biosensors, immobilising the surface of CNTs with some functional groups [10, 23]. However, the biocompatibility of CNTs may also become an important factor considering the shape of CNTs; e.g., needle-like nanomaterials may in general deteriorate the bioactivities [24, 25, 26]. It is known that the affinity of C_{60} fullerene molecules with cells is higher than that of CNTs [27, 28] and therefore C_{60} fullerene molecules have been actively investigated aiming to utilise them in biomedical studies [29, 30, 31, 32].

Here, we synthesise fibres composed of C_{60} molecules and sulphur by dispersing C_{60} and sulphur in benzene and evaporating a droplet of the solution on a substrate. Clusters composed of radially grown fibres are evenly formed on the substrate. We then immobilise the surface of the fibres with a primary antibody; i.e., epithelial cell adhesion molecules (anti-EpCAM), to trap target cells such as TE2 esophageal and DLD-1 colon cancer cells. We find that the cancer cells are efficiently trapped via the antigen-antibody reaction on the surface of the fibres. Furthermore, those cells trapped by the primary antibody immobilised on the fibres proliferate faster than native cells thanks to anti-EpCAM acting as a growth factor. The present

result suggests that different types of cells can be trapped and proliferated on nano fibres by immobilising appropriate antibody molecules on the surface of the fibres.

2. Materials and methods

2.1. Synthesis and characterisation of nano fibres

C_{60} molecules and sulphur were dissolved in 4.52 mL of benzene. The concentration of C_{60} molecules and sulphur was, respectively, set at 1.2 and 6.2 µmol mL^{-1}. The solution was sonicated for 5 min at 20 °C and 1 atm [33]. 100 µL of the solution was dropped onto the surface of a square glass substrate of $18 \times 18 \times 0.17$ (thickness) mm, the temperature of which had been set at 75 °C using a heater installed at the bottom of the substrate. Note that the surface of the glass substrates, which had not been modified with any chemicals, was washed with ethanol before dropping a droplet of the solution onto it. The ambient temperature was 20 °C. Nano fibres were formed after the solution had completely evaporated within 30 s. The structure of the fibres was characterised by a scanning electron microscope (SEM) (SU8030, Hitachi Co., Ltd.) and elemental analysis was carried out by energy dispersive X-ray spectrometry (EDS) (X-MAX80, Horiba Ltd.).

2.2. Surface modification of fibres with the primary antibody

The surface of the fibres was modified with the primary antibody; epithelial cell adhesion molecules (anti-EpCAM; clone 1B7) [34], in order to capture target cells; TE2 esophageal and DLD-1 colon cancer cells, following basically the previous procedure [35, 36]. First, the surface of the fibres was modified with 3-mercaptopropyl trimethoxysilane (MPTMS) (Sigma Co., Ltd.) by soaking the fibres in ethanol, in which 4% (v/v) MPTMS was dissolved, for 30 min. Then, the fibres modified with MPTMS (MPTMS/C_{60}-fibres) were coupled with N-maleimidobutyryloxy succinimide ester (GMBS) (Dojindo Co., Ltd.) by placing the MPTMS/C_{60}-fibres in 0.25 mM aqueous solution of GMBS for 1 h. After having been washed 3 times with pure water, the fibres modified with GMBS/MPTMS (GMBS/MPTMS/C_{60}-fibres) were coupled with an anti-EpCAM by soaking the GMBS/MPTMS/C_{60}-fibres in 10 µg mL^{-1} aqueous solution of anti-EpCAM at 4 °C for 12 h, which resulted in the immobilisation of the primary antibody on the GMBS/MPTMS/C_{60}-fibres; that is, C_{60} fibres modified with anti-EpCAM/GMBS/MPTMS (anti-EpCAM/GMBS/MPTMS/C_{60}-fibres) were produced. Note that no streptavidin was used for linking anti-EpCAM to GMBS in the present study. Note also that the effect of the concentration of aqueous solution of anti-EpCAM on the quantity of anti-EpCAM immobilised on the GMBS/MPTMS/C_{60}-fibres was investigated changing the concentration of anti-EpCAM in the solution; 10, 20, 40 and 50 µg mL^{-1}. The anti-EpCAM/GMBS/MPTMS/C_{60}-fibres were washed with phosphate-buffered saline (PBS) to remove an excess

amount of anti-EpCAM, which had not been immobilised on the GMBS/MPTMS/C_{60}-fibres.

2.3. Visualisation of the primary antibody immobilised on the fibres

A secondary antibody; alexa fluor 488-conjugated anti-mouse IgG antibody (Invitrogen Co., Ltd.), was used for visualising the primary antibody; anti-EpCAM, immobilised on the GMBS/MPTMS/C_{60}-fibres. The anti-EpCAM/GMBS/MPTMS/C_{60}-fibres were placed in 10 μg mL^{-1} aqueous solution of alexa fluor 488 so that alexa fluor 488 was attached to anti-EpCAM. The secondary antibody attached to the anti-EpCAM/GMBS/MPTMS/C_{60}-fibres was observed with a confocal laser microscope (A1, Nicon Co., Ltd.) using a laser beam of 488 nm wavelength for the excitation of alexa fluor 488.

2.4. Measurement of the amount of the primary antibody immobilised on fibres using western blotting

Aqueous solution of anti-EpCAM/GMBS/MPTMS/C_{60}-fibres was centrifuged at 10000 rpm for 5 min to separate a pellet composed of anti-EpCAM/GMBS/MPTMS/C_{60}-fibres from the solvent. Anti-EpCAM molecules were detached from anti-EpCAM/GMBS/MPTMS/C_{60}-fibres and extracted from supernatant, adding sodium dodecylsulphate (SDS) sample buffer composed of 4% SDS, 20% glycerol, 0.004% bromophenol blue, 0.125 M Tris-Hcl and 10% 2-mercaptoethanol to the fibres and supernatant and heating them at 95 °C for 5 min. Anti-EpCAM molecules were then separated via electrophoresis in 10% SDS-polyacrylamide gel for 30 min. Anti-EpCAM was transcribed from the gel to polyvinylidene difluoride membranes using wet type blotting. The membranes were blocked using blocking buffer (Toyobo Co., Ltd.) for 1 h at room temperature. Anti-HRP-conjugated anti-mouse IgG antibody molecules (GE Health Care Bioscience Co., Ltd.) were attached to anti-EpCAM, which had been transcribed on the membranes, placing the membranes into aqueous solution (Can Get Signal Solution2, Toyobo Co., Ltd.) of anti-HRP-conjugated anti-mouse IgG antibody for 1 h at room temperature. Finally, aqueous solution of HRP chemiluminescence (ECL prime, GE Health Care Bioscience Co., Ltd.) was dropped onto anti-HRP-conjugated anti-mouse IgG antibody, which had been attached to anti-EpCAM. The quantity of the primary antibody; anti-EpCAM, immobilised on GMBS/MPTMS/C_{60}-fibres was finally measured based on the HRP chemiluminescence using a CCD imager (LAS 4000, GE Health Care Bioscience Co., Ltd.).

2.5. Cultivation, visualisation and trapping of cells

Three human cancer cell lines; i.e., TE2 esophageal cancer cell line, DLD-1 colon cancer cell line and IM9 B lymphoblast cell line, were separately cultivated in a medium RPMI-1640 (Sigma Co., Ltd.), which contained 1% glutamine (GlutaMAX, Gibco Co., Ltd.), 1% pyruvate sodium (Gibco Co., Ltd.), 10% fetal bovine serum (FBS, Biohit Co., Ltd.) and 1% penicillin/streptomycin (Penstep, Gibco Co., Ltd.), at 37 °C in an atmosphere of 5% CO_2 and 100% humidity. Note that the affinity of the primary antibody; anti-EpCAM, with TE2 and DLD-1 cells is high, whereas that with IM9 cells is extremely low [36, 37]. 2 mL of trypsin was injected into the media to collect TE2 and DLD-1 cells, while IM9 was collected without trypsin. The nuclei of those cancer cells were dyed by soaking the cells in 1 µg mL^{-1} aqueous solution of Hoechst 33342 (Dojindo Co., Ltd.) at 37 °C for 15 min to visualise the cells. A solution of 10000 cells dispersed in 100 µL PBS was dropped onto the anti-EpCAM/GMBS/MPTMS/C_{60}- fibres placed on the substrate and left for 1 h at 37 °C. Note that the solution of the cells was also dropped onto the fibres without any surface modification and the substrate, on which no fibres were placed. Note also that two types of substrates were prepared; (1) the surface of the substrate was immobilised with anti-EpCAM/GMBS/MPTMS following the same procedure explained above; and (2) the surface of the substrate was immobilised only with GMBS/MPTMS. Then, the anti-EpCAM/GMBS/MPTMS/ C_{60}-fibres and the substrate were washed with PBS three times to remove cells, which had not been trapped by the fibres and substrate. 10 µg mL^{-1} aqueous solution of the secondary antibody; Alexa fluor 488, was dropped onto the fibres and substrates for visualising the anti-EpCAM, which had not captured the cells. After having been rinsed with PBS three times, the above cells captured by the primary antibody were placed into 4% aqueous solution of paraformaldehyde for 20 min to protect the cell membranes and then rinsed with PBS three times. Finally, cells captured by the primary antibody on the fibres and substrates were observed with a confocal laser microscope with a laser of 405 nm wavelength (A1, Nicon Co., Ltd.). The number of cells, which had been captured by the primary antibody, was counted from five different images of 261×261 µm^2 located in the central region of the substrate by image software (ImageJ, Freeware) and the number density of the trapped cells was calculated dividing the number of cells trapped on the fibres by the two-dimensional surface area corresponding to the images [38, 39]. The significant difference in the number density of TE2, DLD-1 and IM9 cells trapped onto the fibres and substrates was evaluated by one-way analysis of variance (one-way ANOVA) setting the significant level at 0.01 (StatPlus, Analystsoft Inc.).

2.6. Proliferation of the cells trapped on the fibres

Setting the anti-EpCAM/GMBS/MPTMS/C_{60}-fibres, on which the cells had been trapped, in each well on a 24-well plate and dropping 1 mL of the culture medium into

each well, the cells on the fibres were cultivated in a CO_2 incubator at 37 °C in the atmosphere of 5% CO_2 and 100% humidity for 24, 48 and 72 h. 100 µL of reagent; cell counting kit-8 (Dojin Co., Ltd), having been dropped into each well after incubation, the 24-well plate was placed in the CO_2 incubator for 3 h. Then, the number of cells grown after 24, 48 and 72 h was evaluated measuring the absorbance of photons of 450 nm wavelength with a microplate reader, noting that the absorbance of photons of 600 nm was subtracted as the background from that of 450 nm. The growth of cells on substrates and in the presence of fibres without any surface modification was also measured following the same procedure as described above. Statistical analysis was performed using the one-way ANOVA (StatPlus, Analystsoft Inc.) and the significant level was set at 0.01. The results were presented as mean ± standard deviation.

3. Results and discussion

100 µL of the solution of C_{60} and sulphur dissolved in benzene was dropped onto the glass substrate, the temperature of which had been set at 75 °C, as mentioned, and we found that fibres were formed by C_{60} and sulphur after the evaporation of benzene. Note that no fibres were grown without sulphur [40, 41] and therefore it is supposed that mixing sulphur and C_{60} with the solvent is essential for the formation of fibres [33]. SEM images and EDS mappings of the fibres are shown in Fig. 1. Fibres grew from core seeds in radial directions and clusters composed of fibres were evenly formed on the substrate. The length and width of each fibre were, respectively, of the order of 10 µm and 100 nm. In our previous study, in which case the concentration of C_{60} molecules and sulphur was set at 0.6 and 3.1 µmol mL^{-1} and the surface temperature of the substrate was lower than 50 °C, highly aligned C_{60} fullerene nano fibres were grown in perpendicular directions along the circumference of a droplet via the coffee ring effect [33], noting that no fibres were formed in the central part of the substrate. In the present study, on the contrary, fibres were synthesised in the droplet during the evaporation process and finally deposited evenly on the surface of the substrate due to the relatively high concentration of C_{60} molecules and sulphur; 1.2 and 6.2 µmol mL^{-1}, and high evaporation rate; i.e., the substrate temperature was set at 75 °C.

Confocal laser microscopic images of the secondary antibody; Alexa fluor 488, which was attached to the primary antibody; anti-EpCAM, are shown in Fig. 2. Note that almost all of the primary antibody in the solution was immobilised on the fibres when the fibres were soaked in 10 µg mL^{-1} aqueous solution of the primary antibody (see Fig. 3 for the effect of the initial concentration of aqueous solution of the primary antibody on the quantity of the primary antibody immobilised on the fibres, which was measured by western blotting). It is clearly shown that the primary antibody was uniformly immobilised on the C_{60} fibres. We suppose that GMBS was immobilised on MPTMS via a reaction between sulphhydryl group in MPTMS and maleimide in GMBS, whereas anti-EpCAM was successfully
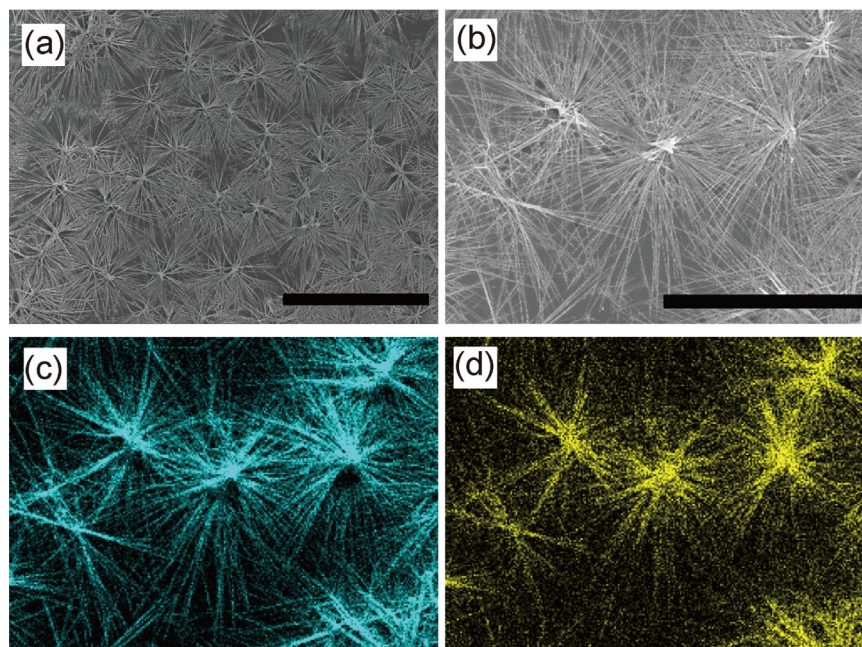
Fig. 1. SEM images and EDS mappings of fibres. (a) SEM image of fibres. The scale bar represents 100 μm. (b) SEM image of fibres. The scale bar represents 60 μm. (c) EDS mapping of carbon corresponding to (b). (d) EDS mapping of sulphur corresponding to (b). The fibres were composed of C_{60} and sulphur.

immobilised on GMBS via a bond between amine in anti-EpCAM and *N*-hydroxysuccinimide in GMBS. We believe that the present anti-EpCAM immobilisation procedure without using streptavidin significantly reduces some cumbersome process and the immobilisation time.

Confocal laser microscopic images of cells trapped on the surface of the fibres, which were modified with the primary antibody, are shown in Fig. 4, where blue and green, respectively, represent the nuclei of cells and the secondary antibody attached to the primary antibody on the fibres. It is supposed that both TE2 esophageal and DLD-1 colon cancer cells were firmly trapped on the surface of the fibres thanks to the primary antibody, considering that neither the cells trapped by anti-EpCAM nor anti-EpCAM itself were removed after the cells and fibres having been rinsed three times with PBS. The number density of cells trapped on fibres and substrates is shown in Fig. 5. The number density of TE2 esophageal and DLD-1 colon cancer cells trapped on the anti-EpCAM/GMBS/MPTMS/C_{60}-fibres and anti-EpCAM/GMBS/MPTMS/substrates was higher than that of IM9 B lymphoblast cells since the affinity of the primary antibody with TE2 and DLD-1 is much higher than that of IM9 [34, 37, 38], and that the number density of the cells trapped on fibres and substrates with surface modification with the primary antibody is much higher than that without any surface modification. It is clearly shown that the augmentation of the surface area of materials and modification of
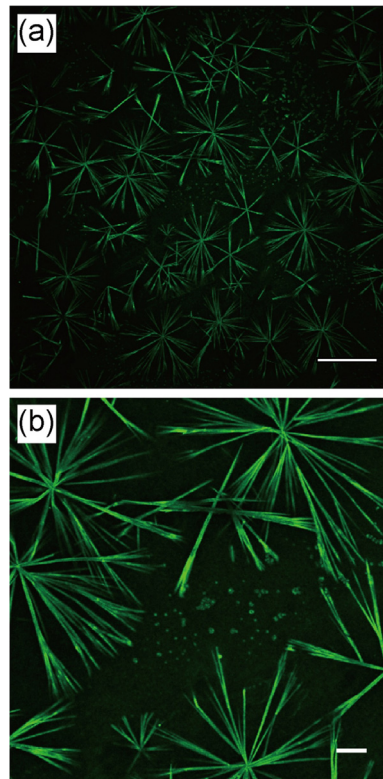
Fig. 2. Confocal laser microscopic images of the primary antibody; anti-EpCAM, immobilised on the surface of fibres. The secondary antibody; alexa fluor 488, which had been attached to the primary antibody, was visualised using a laser beam of 488 nm wavelength. The scale bar in image (a) and (b), respectively, represents 50 and 10 μm.
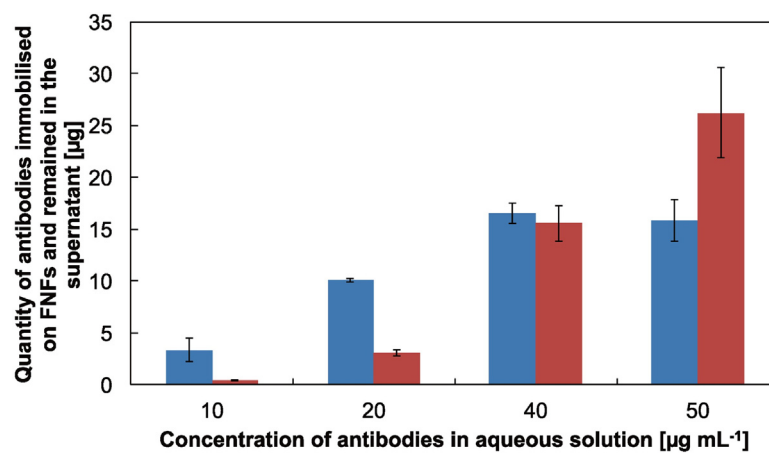

Fig. 3. Effect of the initial concentration of aqueous solution of the primary antibody; anti-EpCAM, on the quantity of the primary antibody immobilised on the surface of fibres. Blue bar: Quantity of the primary antibody immobilised on the surface of fibres; Red bar: Quantity of the primary antibody remained in the supernatant.
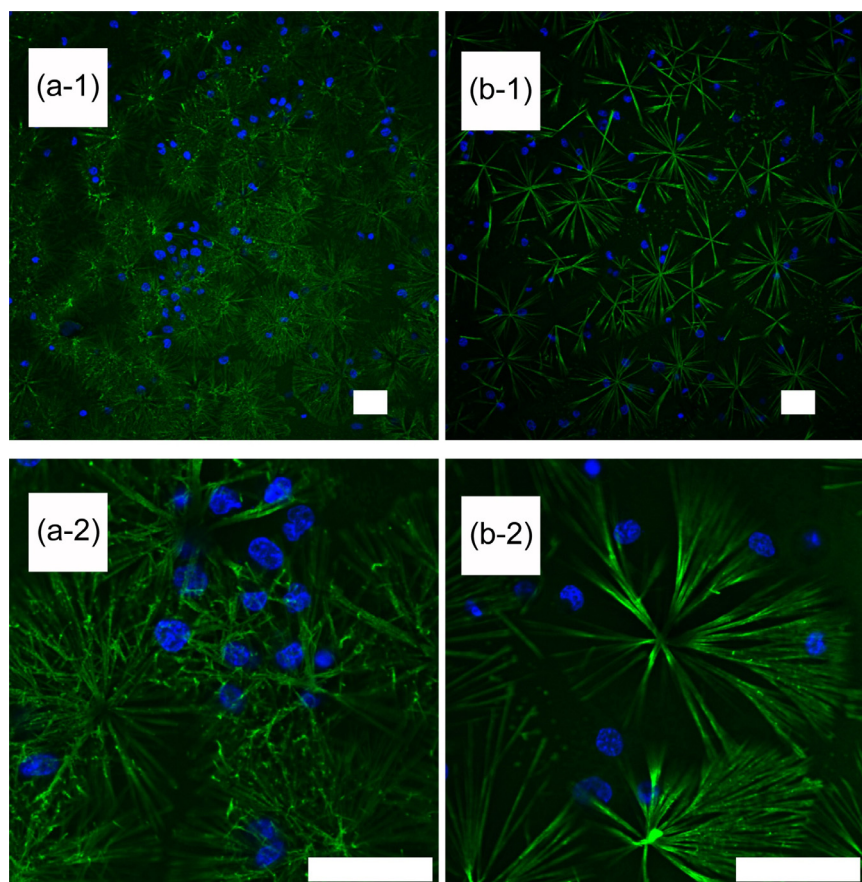
Fig. 4. Confocal laser microscopic images of the primary antibody; anti-EpCAM, immobilised on the surface of fibres and cells trapped by the primary antibody immobilised on fibres. (a-1) Low magnification image of TE2 cells trapped on fibres. The scale bar represents 100 μm. (a-2) High magnification image of TE2 cells trapped on fibres. The scale bar represents 10 μm. (b-1) Low magnification image of DLD-1 cells trapped on fibres. The scale bar represents 100 μm. (b-2) High magnification image of DLD-1 cells trapped on fibres. The scale bar represents 10 μm. Green colour represents the primary antibody, whereas blue the nuclei of the cancer cells.

the surface of materials with a specific antibody possessing a high affinity with target cells greatly improved the trapping efficiency of the target cells.

It is important to know whether the cells trapped on the anti-EpCAM/GMBS/MPTMS/C_{60}-fibres will proliferate or not. If the cells on the fibres grow, detailed analysis and characterisation of the cells can be carried out, which may make it possible to detect and examine even an extremely small number of cells existing in sample fluids. In the present study, two types of cells; TE2 and DLD-1, which had been trapped on the anti-EpCAM/GMBS/MPTMS/C_{60}-fibres, were cultivated as explained in the previous section. The proliferation of TE2 and DLD-1 cells trapped on the fibres, which had been immobilised with antibody; anti-EpCAM, and IM9 cells in the presence of fibres is shown in Fig. 6, where the growth of the cells in the presence of fibres without any surface modification and the native cells
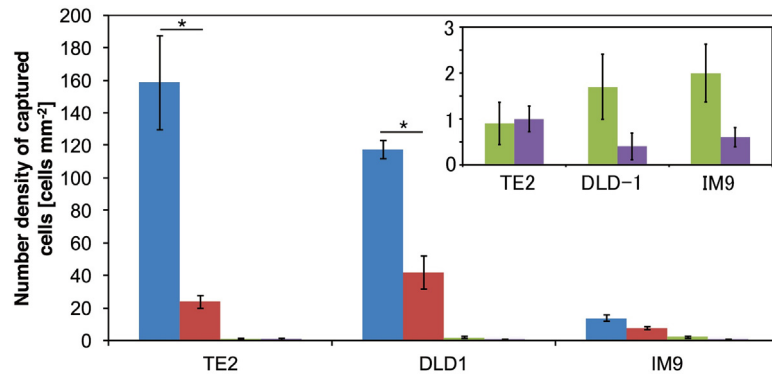
Fig. 5. Number density of TE2 esophageal cancer cells, DLD-1 colon cancer cells and IM9 B lymphoblast cells trapped on the surface of fibres and substrates. Those cells trapped on the surface of fibres and substrates without any surface modification are shown in the inset. Blue bar: Number density of cells trapped on the surface of fibres modified with the primary antibody; Red bar: Number density of cells trapped on the surface of glass substrates modified with the primary antibody; Green bar: Number density of cells trapped on the surface of fibres without any primary antibody; Purple bar: Number density of cells trapped on the surface of glass substrates without any primary antibody.

in the absence of the fibres is also represented as a control. The growth rate of both TE2 and DLD-1 cells trapped on the antibody, which had been immobilised on the fibres, was higher than that in the presence of fibres without any surface modification and the native ones in the absence of fibres, which confirms that the antibody; anti-EpCAM, worked as a cells' growth factor [42] as well as cell capturing molecules.

We demonstrated using TE2 esophageal, DLD-1 colon cancer and IM9 B lymphoblast cells as model ones that target cells; that is, TE2 and DLD-1 cells, were successfully trapped on fibres, which had been immobilised with a specific antibody; anti-EpCAM. The present result shows that different types of cells can be efficiently captured using nano fibres by immobilising the surface of the fibres with specific antibodies possessing high affinities with target cells. What is more, the trapped cells proliferated thanks to the antibody; anti-EpCAM, acting as a growth factor, which suggests that even an extremely small number of cells such as circulating tumour cells (CTCs) in blood may be detected in the early stage of cancer spread since the number of cells can be increased after target cells having been trapped using fibres, on which antibody molecules are immobilised. In terms of practicality, the fibres may also be used for capturing obstacle cells such as white and red blood cells in advance and then CTCs may be trapped by setting a series of fibres. Note that the present synthetic methodology is advantageous in such a sense that fibres can be instantly grown anywhere on the surface of substrates. We will be developing some practical methodologies for trapping and characterising an extremely small number of target cells such as CTCs in sample fluids using the present hybrid fibres.
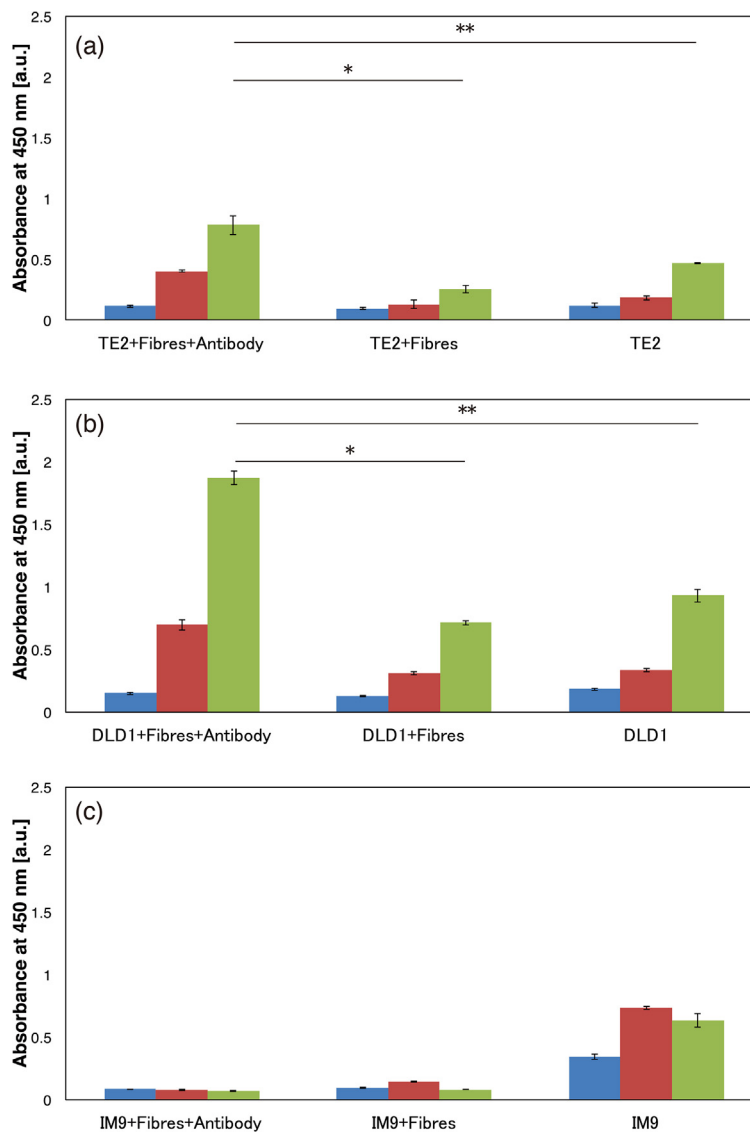
Fig. 6. Growth of TE2 esophageal and DLD-1 colon cancer cells and IM9 B lymphoblast cells. The growth of cells in the presence of fibres with/without surface modification and native cells in the absence of fibres is shown. (a) Growth of TE2 cells; (b) Growth of DLD-1 cells; (c) Growth of IM9 cells. Blue bar: Growth of cells after 24 h cultivation; Red bar: 48 h; Green bar: 72 h. The growth rate of TE2 and DLD-1 cells trapped by the primary antibody, which was immobilised on the fibres, is higher than that in the presence of fibres without any surface modification and native cells. The growth of IM9 cells was suppressed in the absence of fibres with/without surface modification with the primary antibody.

4. Conclusions

We synthesised fibres composed of C_{60} and sulphur by dropping a droplet of a solution of C_{60} and sulphur dissolved in benzene and evaporating the droplet on a substrate. The synthetic methodology is so simple that fibres can be formed within 30 s on any area on a substrate/device. The surface of the fibres was immobilised

with the primary antibody to trap target cells. We finally trapped TE2 esophageal and DLD-1 colon cancer cells on the fibres. We demonstrated that the number of captured target cells was greatly increased using the nano fibres, the surface of which was immobilised with a specific antibody. We also investigated the proliferation of TE2 and DLD-1 cells trapped on the antibody, which had been immobilised on the surface of the fibres, and found that the growth rate of the cells trapped on the anti-EpCAM/GMBS/MPTMS/C_{60}-fibres was higher than that of the native cells. The present result suggests that different types of cells and biomolecules can be trapped on nano fibres by immobilising appropriate antibody molecules on the surface of the fibres and that the cells can be grown on the fibres for further analysis and characterisation of the cells for the detection of diseases. What is more, the present methodology may well be utilised for the capture of exosomes discharged from cancer cells for the detection of cancer in the early stage, considering that a number of exosomes is discharged from each circulating tumour cell [43, 44].

Declarations

Author contribution statement

Seiki Iwai: Conceived and designed the experiments; Analyzed and interpreted the data; Wrote the paper.

Shunji Kurosu: Performed the experiments; Analyzed and interpreted the data.

Hideki Sasaki: Performed the experiments.

Kazunori Kato: Analyzed and interpreted the data; Contributed reagents, materials, analysis tools or data.

Toru Maekawa: Conceived and designed the experiments; Analyzed and interpreted the data; Contributed reagents, materials, analysis tools or data; Wrote the paper.

Funding statement

Competing interest statement

The authors declare no conflict of interest.

Additional information

No additional information is available for this paper.

References

[1] C.J. Hawker, T.P. Russell, Block Copolymer Lithography: Merging 'Bottom-Up' with 'Top-Down' Processes, MRS Bull. 30 (2005) 952–966.

[2] D.L. Elbert, Bottom-up tissue engineering, Curr. Opin. Biotechnol. 22 (2011) 674–680.

[3] A. Biswas, I.S. Bayer, A.S. Biris, T. Wang, E. Dervishi, F. Faupel, Advances in top-down and bottom-up surface nanofabrication: Techniques applications & future prospects, Adv. Colloid Interface Sci. 170 (2012) 2–27.

[4] S. Watanabe, K. Inukai, S. Mizuta, M.T. Miyahara, Mechanism for stripe pattern formation on hydrophilic surfaces by using convective self-assembly, Langmuir 25 (2009) 7287–7295.

[5] Y. Mino, S. Watanabe, M.T. Miyahara, Fabrication of colloidal grid network by two-step convective self-assembly, Langmuir 27 (2011) 5290–5295.

[6] P.J. Yunker, T. Still, M.A. Lohr, A.G. Yodh, Suppression of the coffee-ring effect by shape-dependent capillary interactions SI, Nature 476 (2011) 308–311.

[7] M. Anyfantakis, Z. Geng, M. Morel, S. Rudiuk, D. Baigl, Modulation of the coffee-ring effect in particle/surfactant mixtures: The importance of particle-interface interactions, Langmuir 31 (2015) 4113–4120.

[8] B.J. Jankiewicz, D. Jamiola, J. Choma, M. Jaroniec, Silica-metal core-shell nanostructures, Adv. Colloid Interface Sci. 170 (2012) 28–47.

[9] K. Stephansen, M. Mattebjerg, J. Wattjes, A. Milisavljevic, F. Jessen, K. Qvortrup, F.M. Goycoolea, I.S. Chronakis, Design and characterization of self-assembled fish sarcoplasmic protein-alginate nanocomplexes, Int. J. Biol. Macromol. 76 (2015) 146–152.

[10] A. Abarrategi, M.C. Gutiérrez, C. Moreno-Vicente, M.J. Hortigüela, V. Ramos, J.L. López-Lacomba, M.L. Ferrer, F. del Monte, Multiwall carbon nanotube scaffolds for tissue engineering purposes, Biomaterials 29 (2008) 94–102.

[11] A.C. Poulose, S. Veeranarayanan, M.S. Mohamed, Y. Sakamoto, N. Hirosawa, Y. Suzuki, M. Zhang, M. Yudasaka, N. Radhakrishnan, T. Maekawa, P.V. Mohanan, D. Sakthi Kumar, Characterizing the

biocompatibility and tumor-imaging capability of Cu $_2$ S nanocrystals in vivo, Nanoscale 7 (2015) 13061–13074.

[12] M.K. Shin, S.I. Kim, S.J. Kim, S.Y. Park, Y.H. Hyun, Y. Lee, K.E. Lee, S.S. Han, D.P. Jang, Y.B. Kim, Z.H. Cho, I. So, G.M. Spinks, Controlled magnetic nanofiber hydrogels by clustering ferritin, Langmuir 24 (2008) 12107–12111.

[13] N. Zhang, Y. Deng, Q. Tai, B. Cheng, L. Zhao, Q. Shen, R. He, L. Hong, W. Liu, S. Guo, K. Liu, H.R. Tseng, B. Xiong, X.Z. Zhao, Electrospun TiO$_2$ nanofiber-based cell capture assay for detecting circulating tumor cells from colorectal and gastric cancer patients, Adv. Mater. 24 (2012) 2756–2760.

[14] T.C. Lin, F.H. Lin, J.C. Lin, In vitro feasibility study of the use of a magnetic electrospun chitosan nanofiber composite for hyperthermia treatment of tumor cells, Acta Biomater. 8 (2012) 2704–2711.

[15] S. Van Bael, Y.C. Chai, S. Truscello, M. Moesen, G. Kerckhofs, H. Van Oosterwyck, J.P. Kruth, J. Schrooten, The effect of pore geometry on the in vitro biological behavior of human periosteum-derived cells seeded on selective laser-melted Ti6Al4 V bone scaffolds, Acta Biomater. 8 (2012) 2824–2834.

[16] S. He, T. Xia, H. Wang, L. Wei, X. Luo, X. Li, Multiple release of polyplexes of plasmids VEGF and bFGF from electrospun fibrous scaffolds towards regeneration of mature blood vessels, Acta Biomater. 8 (2012) 2659–2669.

[17] H.N. Chia, M. Vigen, A.M. Kasko, Effect of substrate stiffness on pulmonary fibroblast activation by TGF-β, Acta Biomater. 8 (2012) 2602–2611.

[18] D. Kai, M.P. Prabhakaran, G. Jin, S. Ramakrishna, Biocompatibility evaluation of electrically conductive nanofibrous scaffolds for cardiac tissue engineering, J. Mater. Chem. B (2013).

[19] J.-H. Kim, F.A. Sheikh, H.W. Ju, H.J. Park, B.M. Moon, O.J. Lee, C.H. Park, 3D silk fibroin scaffold incorporating titanium dioxide (TiO2) nanoparticle (NPs) for tissue engineering, Int. J. Biol. Macromol. 68 (2014) 158–168.

[20] Q. Zhang, S. Lv, J. Lu, S. Jiang, L. Lin, Characterization of polycaprolactone/collagen fibrous scaffolds by electrospinning and their bioactivity, Int. J. Biol. Macromol. 76 (2015) 94–101.

[21] K. Donaldson, R. Aitken, L. Tran, V. Stone, R. Duffin, G. Forrest, A. Alexander, Carbon nanotubes: A review of their properties in relation to pulmonary toxicology and workplace safety, Toxicol. Sci. 92 (2006) 5–22.

[22] J.W. Nichol, A. Khademhosseini, Modular Tissue Engineering: Engineering Biological Tissues from the Bottom Up, Soft Matter 5 (2009) 1312–1319.

[23] W. Yang, K.R. Ratinac, S.R. Ringer, P. Thordarson, J.J. Gooding, F. Braet, Carbon nanomaterials in biosensors: Should you use nanotubes or graphene, Angew. Chemie − Int. Ed. 49 (2010) 2114–2138.

[24] C.-W. Lam, J.T. James, R. McCluskey, S. Arepalli, R.L. Hunter, A review of carbon nanotube toxicity and assessment of potential occupational and environmental health risks, Crit. Rev. Toxicol. 36 (2006) 189–217.

[25] S.K. Smart, A.I. Cassady, G.Q. Lu, D.J. Martin, The biocompatibility of carbon nanotubes, Carbon 44 (2006) 1034–1047.

[26] J. Palomäki, E. Välimäki, J. Sund, M. Vippola, P.A. Clausen, K.A. Jensen, K. Savolainen, S. Matikainen, H. Alenius, Long, needle-like carbon nanotubes and asbestos activate the NLRP3 inflammasome through a similar mechanism, ACS Nano 5 (2011) 6861–6870.

[27] T. Da Ros, M. Prato, Medicinal chemistry with fullerenes and fullerene derivatives, Chem. Commun. 66 (1999) 3–66 9.

[28] N. Saleh, A. Afrooz, J. Bisesi Jr., N. Aich, J. Plazas-Tuttle, T. Sabo-Attwood, Emergent Properties and Toxicological Considerations for Nanohybrid Materials in Aquatic Systems, Nanomaterials 4 (2014) 372–407.

[29] S. Bosi, T. Da Ros, G. Spalluto, M. Prato, Fullerene derivatives: an attractive tool for biological applications, Eur. J. Med. Chem. 38 (2003) 913–923.

[30] C.M. Sayes, A.M. Gobin, K.D. Ausman, J. Mendez, J.L. West, V.L. Colvin, Nano-C60 cytotoxicity is due to lipid peroxidation, Biomaterials 26 (2005) 7587–7595.

[31] G. Jia, H. Wang, L. Yan, X. Wang, R. Pei, T. Yan, Y. Zhao, X. Guo, Cytotoxicity of carbon nanomaterials: Single-wall nanotube, multi-wall nanotube, and fullerene, Environ. Sci. Technol. 39 (2005) 1378–1383.

[32] K. Kümmerer, J. Menz, T. Schubert, W. Thielemans, Biodegradability of organic nanoparticles in the aqueous environment, Chemosphere 82 (2011) 1387–1392.

[33] S. Kurosu, T. Fukuda, T. Maekawa, Quick synthesis of highly aligned or randomly oriented nanofibrous structures composed of C_{60} molecules via self-assembly, Adv. Nat. Sci. Nanosci. Nanotechnol. 4 (2013) 25003.

[34] K. Suzuki, K. Nakamura, K. Kato, H. Hamada, T. Tsukamoto, Exploration of target molecules for prostate cancer gene therapy, Prostat. 67 (2007) 1163–1173.

[35] S. Nagrath, L.V. Sequist, S. Maheswaran, D.W. Bell, D. Irimia, L. Ulkus, M. R. Smith, E.L. Kwak, S. Digumarthy, A. Muzikansky, P. Ryan, U.J. Balis, R.

G. Tompkins, D.A. Haber, M. Toner, Isolation of rare circulating tumour cells in cancer patients by microchip technology, Nature 450 (2007) 1235–1239.

[36] T. Yamashita, J. Ji, A. Budhu, M. Forgues, W. Yang, H.-Y. Wang, H. Jia, Q. Ye, L.-X. Qin, E. Wauthier, L.M. Reid, H. Minato, M. Honda, S. Kaneko, Z.-Y. Tang, X.W. Wang, EpCAM-positive hepatocellular carcinoma cells are tumor-initiating cells with stem/progenitor cell features, Gastroenterology 136 (2009) 1012–1024.

[37] C. Patriarca, R.M. Macchi, A.K. Marschner, H. Mellstedt, Epithelial cell adhesion molecule expression (CD326) in cancer: a short review, Cancer Treat. Rev. 38 (2012) 68–75.

[38] C.A. Schneider, W.S. Rasband, K.W. Eliceiri, NIH Image to ImageJ: 25 years of image analysis, Nature Methods 9 (2012) 671–675.

[39] P. Choudhry, High-Throughput method for automated colony and cell counting by digital image analysis based on edge detection, PLoS One 11 (2016) e0148469.

[40] L.I. Buravov, O.A. D'yachenko, S.V. Konovalikhin, N.D. Kushch, I.P. Lavrent'ev, N.G. Spitsyna, G.V. Shilov, E.B. Yagubskii, A complex of buckminsterfullerene with sulfur, $C_{60} \bullet 2S_8$: synthesis and crystal structure, Russ. Chem. Bull. 43 (1994) 240–244.

[41] M.-F. Gardette, A. Chilouet, S. Toscani, H. Allouchi, V. Agafonov, J.-C. Rouland, H. Szwarc, R. Céolin, Phase equilibria in the C_{60}-sulphur system, Chem. Phys. Lett. 306 (1999) 149–154.

[42] M. Balzar, I.H. Briaire-de Bruijn, H.A.M. Rees-Bakker, F.A. Prins, W. Helfrich, L. de Leij, C. Riethmüller, S. Alberti, S.O. Warnaar, G.J. Fleuren, S. V. Litvinov, Epidermal growth factor-like repeats mediate lateral and reciprocal interactions of Ep-CAM molecules in homophilic adhesions, Mol. Cell. Biol. 21 (2001) 2570–2580.

[43] K. Denzer, M.J. Kleijmeer, H.F. Heijnen, W. Stoorvogel, H.J. Geuze, Exosome: from internal vesicle of the multivesicular body to intercellular signaling device, J. Cell Sci. 113 (Pt 19) (2000) 3365–3374.

[44] J.L. Hood, S. San Roman, S.A. Wickline, Exosomes released by melanoma cells prepare sentinel lymph nodes for tumor metastasis, Cancer Res. 71 (2011) 3792–3801.